BMB
reports

Biochemical characterization of the lipid-binding properties of a broccoli cuticular wax-associated protein, WAX9D, and its application

Sunyoung Ahn[#], Jongmin Kim[#], Jaeho Pyee & Heonyong Park[*]

Department of Molecular Biology and Institute of Nanosensor and Biotechnology, BK21 Graduate Program for RNA Biology, Dankook University, Yongin 448-701, Korea

In this study, we showed that WAX9D, a nonspecific lipid-transfer protein found in broccoli, binds palmitate (C16) and stearate (C18) with dissociation constants of 0.56 μM and 0.52 μM, respectively. WAX9D was fused to thioredoxin protein by genetic manipulation to enhance its solubility. The data revealed strong interaction of Trx-WAX9D with palmitate and stearate. The dissociation constants of Trx-WAX9D for palmitate and stearate were 1.1 μM and 6.4 μM, respectively. The calculated number of binding sites for palmitate and stearate was 2.5 to 2.7, indicating that Trx-WAX9D can bind three molecules of fatty acids. Additionally, Trx-WAX9D was shown to inhibit the apoptotic effect of palmitate in endothelial cells. Our data using Trx-WAX9D provide insight into the broad spectrum of its biological applications with specific palmitate binding. [BMB reports 2009; 42(6): 367-372]

INTRODUCTION

Nonspecific lipid-transfer proteins (nsLTPs) are present in a variety of plants, including maize, barley, rice, and broccoli (*Brassica oleracea*). They are known to facilitate the intermembrane transfer of various lipids (1). The lipid-transfer activity of nsLTPs has been proposed to play an important role in the formation of a hydrophobic wax layer on the plant cell surface that provides a defense against fungal and bacterial growth (2, 3). The three-dimensional (3-D) structures of a variety of plant nsLTPs were determined previously by X-ray crystallography and nuclear magnetic resonance spectroscopy (4-7). Comparison of these 3-D structures has revealed two consensus sequences located in the C-terminal hydrophobic cavity that contribute to lipid binding, namely, T/S-X-X-D-R/K and P-Y-X-I-S (8). The tyrosine residue in the lipid-binding cavity facilitates monitoring of lipid binding through its intrinsic fluorescence (9). Therefore, fluorescence spectroscopy has been used to characterize the lipid-binding properties of nsLTPs (10).

WAX9D (Gene ID: L33907), the major protein in the cuticular wax of broccoli leaves, is localized to the outer surface of the epidermis, as well as other tissues, including the mesophyll and xylem (11). Composed of 118 residues, the amino acid sequence of WAX9D shows a high degree of homology with other nsLTPs. Due to its highly homologous sequence, WAX9D has been proposed to interact with a variety of fatty acids. However, the lipid-binding activities of WAX9D remain unknown.

In the current study, we determined the *in vitro* fatty acid-binding activity of the broccoli WAX9D by intrinsic fluorescence spectroscopy. The data presented here also provide insight into the *in vivo* functions of WAX9D and the diversity of biological applications for the recombinant WAX9D protein.

RESULTS

Fatty acid binding of WAX9D

WAX9D was isolated from broccoli leaves by extraction with an organic solvent [chloroform : methanol, 2 : 1 (v/v)]. Bands corresponding to the WAX9D protein appeared homogeneous in SDS-PAGE and native gel electrophoresis (Fig. 1), indicating that the purity of extracted WAX9D was extremely high. The molecular weight of WAX9D could not be estimated accurately by these electrophoretic data due to band compression of proteins smaller than 11 kDa.

Fatty acid binding experiments for broccoli WAX9D was performed by assessing the intrinsic fluorescence of tyrosine. Based on sequence alignment with other nsLTPs, broccoli WAX9D may possess a tyrosine residue in the central pore (data not shown) that most likely monitors the environmental change of tyrosine in the central pore according to lipid binding. As shown in Fig. 2A, when a small amount of palmitate (C16) was added to broccoli WAX9D, the tyrosine fluorescence decreased significantly. However, the additions of myristate and other saturated fatty acids (C10 to C14) had no effect on tyrosine fluorescence (Fig. 2B and C), indicating that short-length fatty acids either do not bind broccoli WAX9D or that their binding may

*Corresponding author. Tel: 82-31-8005-3193; Fax: 82-31-8005-3191; E-mail: heonyong@dankook.ac.kr
[#]Authors contributed equally to this work.

Received 15 October 2008, Accepted 3 January 2009

Keywords: Apoptosis, Binding, Fatty acids, Fluorescence spectroscopy, Lipid-transfer proteins

not be detected by tyrosine fluorescence. For palmitate and stearate (C18) binding assays, saturation was reached at a ligand-to-protein ratio greater than 1. Therefore, for convenience in data fitting, we used a simple multiple ligand-binding model, called the all-or-none ligand-binding model, in which there are only two WAX9D protein species, the free and ligand-saturated forms. This data fitting procedure generated dissociation constants (K_d) and the number of binding sites (n) of broccoli WAX9D for palmitate and stearate. The K_d values for palmitate and stearate were 0.56 ± 0.09 μM and 0.52 ± 0.03 μM, respectively. The number of binding sites for palmitate and stearate were 1.48 ± 0.32 and 1.74 ± 0.15, respectively.

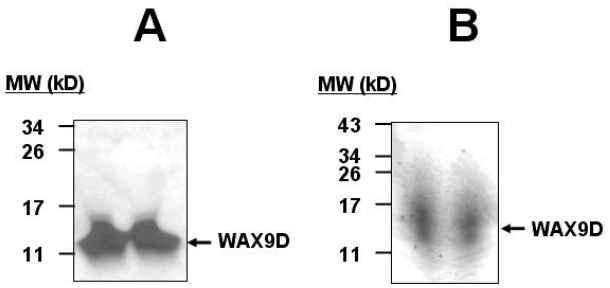

Fig. 1. Native WAX9D is a major protein in the cuticular wax of broccoli. WAX9D purified from broccoli leaves was resolved by SDS-PAGE. (A) Duplicate samples were resolved by SDS-PAGE then stained with Coomassie Brilliant Blue. (B) Duplicate samples were resolved by native gel electrophoresis then developed by using silver staining.

Solubility results for WAX9D

The limited amount of WAX9D was detected in water-based extraction buffers when WAX9D was extracted from broccoli leaves (data not shown). Thus, we estimated the solubility of WAX9D based on its amino acid sequence using a software program named PROSO (12). Comparison of solubility to other nsLTPs suggested that WAX9D is a water-insoluble protein (data not shown).

To enhance the solubility of WAX9D, we constructed a thioredoxin (Trx)-conjugated WAX9D protein and purified the recombinant *His*-tagged Trx-WAX9D protein from *E. coli* by NTA-Ni^{2+} column chromatography. To obtain untagged WAX9D, Trx-WAX9D-NTA-Ni^{2+} bead complexes were treated with a protease, thrombin, and the thrombin-cleaved protein was eluted. Trx-untagged WAX9D was found predominantly in the insoluble bead fraction, consistent with the finding that WAX9D is extremely water-insoluble (data not shown).

Lipid binding of the Trx-WAX9D protein

Because WAX9D is a water-insoluble protein, its characterization was performed using the soluble, Trx-conjugated form. Structural analyses of other nsLTPs indicate the presence of tyrosine in the central pore, into which fatty acids can be incorporated. Thus, we carried out tyrosine fluorescence spectroscopy to assess the lipid-binding properties of Trx-WAX9D. The protein-intrinsic fluorescence spectra for Trx-WAX9D were

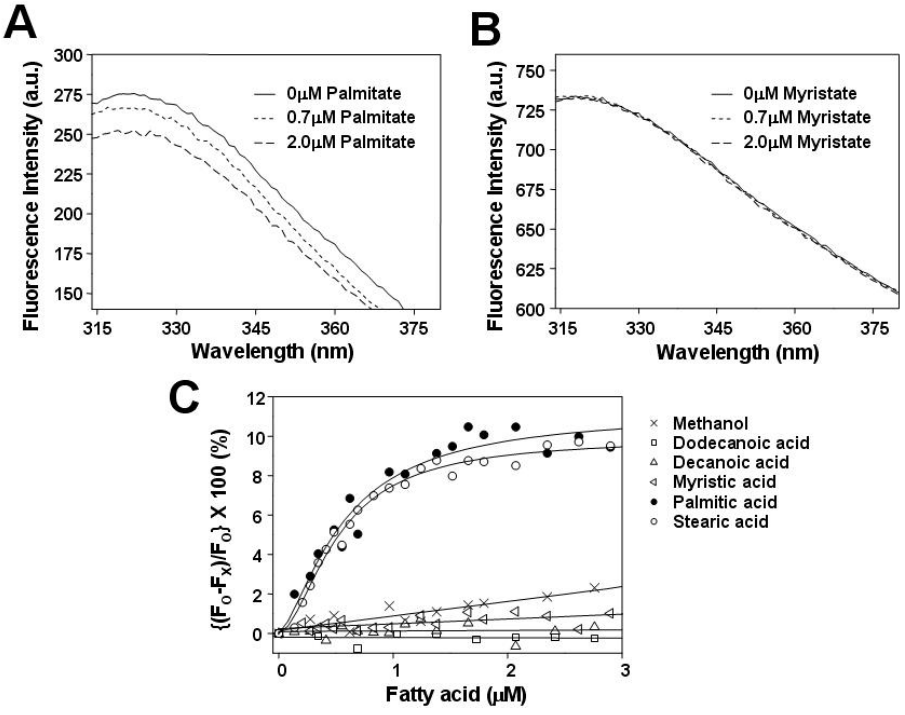

Fig. 2. Fluorescence spectra and lipid-binding properties of broccoli WAX9D at various concentrations of fatty acids. (A) Fluorescence spectra of broccoli WAX9D at various concentrations of palmitate. (B) Fluorescence spectra at diverse myristate concentrations. (C) The F values for broccoli WAX9D were obtained at various concentrations of fatty acids with various chain lengths, C10 (□), C12 (△), C14 (◁), C16 (●), C18 (○), and methanol (×). Data are plotted as a function of fatty acid concentration and the data fits were obtained as described in Materials and Methods.

complex (data not shown); they appeared as a mixture of other types of spectra (for two tryptophans and two tyrosines). To selectively monitor alterations in fluorescence spectra for tyrosine in the binding cavity, we plotted the average wavelength (<λ>) of each spectrum that might have been most affected by changes in hydrophobicity near the tyrosine residue in the binding cavity.

Binding data for palmitic acid were fitted with two different models (Fig. 3A). Scheme I was proposed according to the structural basis for rice nsLTP (13). Rice nsLTP likely binds palmitate in dual lipid-binding modes to one binding pocket. Scheme II represents a simple cooperative binding model expressing a modified Hill equation. Scheme II fit our data better than Scheme I, implying that Trx-WAX9D interacts cooperatively with palmitate. Data from binding experiments with other fatty acids (C10 to C18) and cholesterol were fitted with the equation derived from Scheme II. As shown in Fig. 3B, Trx-WAX9D bound both palmitate and stearate. The binding data also determined that Trx-tagged proteins did not bind palmitate, suggesting the binding specificity of Trx-WAX9D to palmitate. The K_d values for palmitate and stearate were 1.1 ± 0.1 μM and 6.4 ± 0.8 μM, respectively. The number of binding sites for palmitate and stearate were 2.7 ± 0.2 and 2.5 ± 0.5, respectively. Our binding site data indicate that one binding cavity of Trx-WAX9D accommodates binding of three molecules of palmitate or stearate.

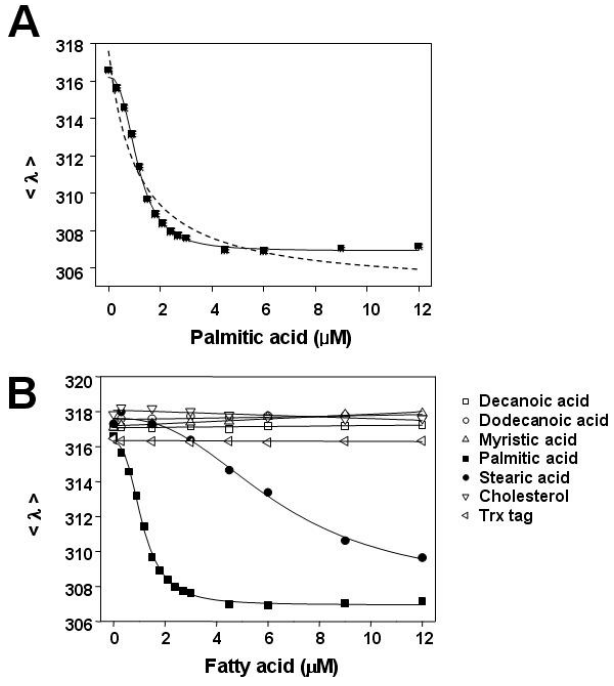

Fig. 3. Binding profiles of Trx-WAX9D with various fatty acids. (A) Average wavelengths (<λ>) of Trx-WAX9D were obtained at various palmitate concentrations, and then the data was fitted according to two different models as described in Materials and Methods. The dotted line represents the best fit obtained with Scheme I and the solid line represents the best fit obtained with Scheme II. (B) Average wavelengths of Trx-WAX9D for fatty acids with various chain lengths, C10 (□), C12 (○), C14 (△), C16 (■), C18 (●), and cholesterol (▽) were obtained and plotted as a function of fatty acid concentration. The <λ> values of Trx-untagged WAX9D (◁) were also obtained as a control.

We also studied the kinetics of palmitate binding to Trx-WAX9D. The kinetic data were fitted to a single exponential equation that revealed two possible scenarios (data not shown). One possibility is that more than two palmitate molecules may be associated simultaneously with a single binding cavity. It is also possible that binding of the first palmitate molecule occurs within 1.2 sec dead time of our time-resolved fluorescence or that binding of the second or third molecules are not detectable. The relaxation time ($t_{1/2}$) was approximately 0.75 ± 0.08 min. The binding rate was slower than that of other nsLTPs; the half-times for lipid binding to maize nsLTP and wheat nsLTP are approximately 2 to 8 sec (14).

Trx-WAX9D reversed the antiapoptotic effect of palmitate

Lipid-binding assays revealed the lipid-binding property of Trx-WAX9D to be different from that of broccoli WAX9D. The dissociation constants and number of lipid-binding sites for Trx-WAX9D were higher than those for broccoli WAX9D. These data indicate that Trx tagging may cause conformational changes leading to alteration in the binding properties of WAX9D. One notable change is the elevated palmitate-binding specificity of Trx-WAX9D. The K_d value for palmitate changed little in Trx-WAX9D, whereas that for stearate decreased 10-fold, indicating that Trx-WAX9D binds palmitate more specifically than stearate. This specific binding property was not found in broccoli WAX9D (Fig. 2) and will be utilized in a broad area of biological applications.

As a biological application of Trx-WAX9D, we tested whether Trx-WA9D reversed the functional activities triggered by palmitate. Data shown in Fig. 4 support previous documentation that palmitate regulates vascular functions (15, 16). Our results also suggest that, due to the elevated palmitate binding specificity, Trx-WAX9D will be utilized more efficiently to inhibit palmitate-induced vascular functions, including vascular cell apoptosis and cell signaling pathways (Fig. 4). Previously, it was documented that p38 mitogen-activated protein kinase mediates the palmitate-induced apoptosis in endothelial cells (15, 16), and this finding consistent with our data. In conclusion, Trx-WAX9D reversed the palmitate-induced vascular activities.

DISCUSSION

WAX9D is found in the surface wax layer of broccoli leaves, and its biological function has yet to be elucidated. Based on its sequence homology to a diversity of nsLTPs, it has been proposed that WAX9D binds and transfers lipids between membranous vesicles. However, there is no evidence of shared functional activities between WAX9D and other nsLTPs.

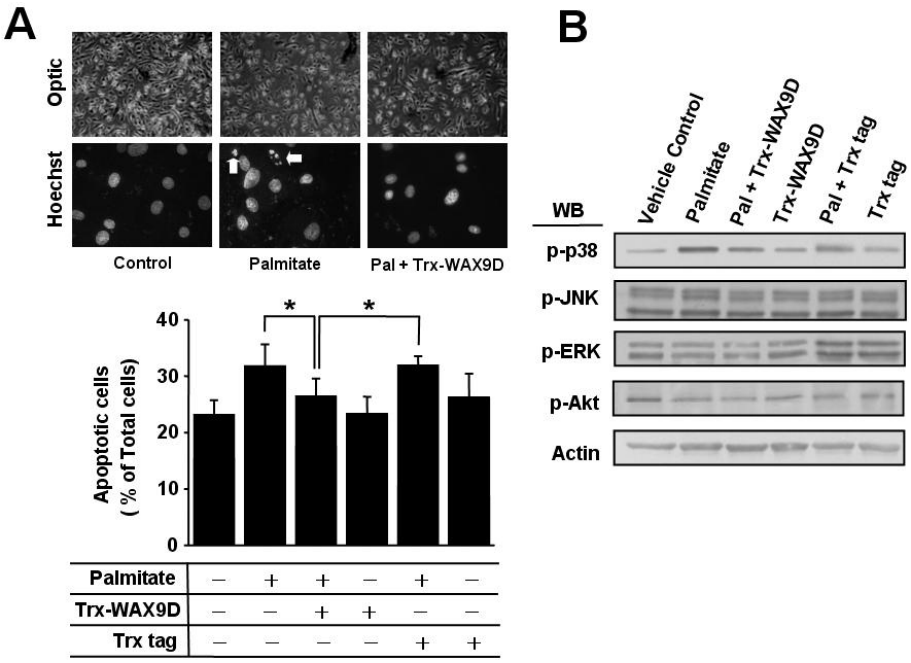

Fig. 4. Trx-Wax9D reversed the effects of palmitate on apoptosis and cell signaling pathways. BAECs were pretreated with 200 μM palmitate, 10 μM Trx, or 10 μM Trx-WAX9D. After 24 hours, the number of apoptotic cells was assessed as described in Materials and Methods. (A) Representative microscopic graphs show the apoptotic round cells observed under an optic microscope and nuclei stained with Hoechst 33258 under a fluorescence microscope. The arrows indicate fragmented nuclei. Quantification was performed by counting the apoptotic cells. The bar graphs represent the percentages of apoptotic cells (mean ± S.E., *$P < 0.01$) (B) Western blots for various signaling molecules. Three independent experiments were performed.

Although our findings have established that WAX9D is a monomeric protein, consistent with the structure of other nsLTPs, we also found that the solubility of WAX9D is extremely low, inconsistent with that of other nsLTPs. A protein's solubility is partly responsible for its functionality *in vivo*. Water-insoluble proteins may be selectively localized in hydrophobic subcellular compartments, including the plasma membrane. Distinct subcellular localization of a protein grants place-associated functionality. The low solubility of WAX9D suggests a difference in functionality *in vivo* compared with other nsLTPs.

One example showing that the lipid-binding property of broccoli WAX9D is distinct from that of other nsLTPs is the narrow binding spectrum of fatty acids. WAX9D binds two fatty acids, palmitate (C16) and stearate (C18), whereas other nsLTPs bind various fatty acids with chain lengths ranging from C12 to C18 (10). On the contrary, the binding properties of broccoli WAX9D for palmitate and stearate parallel those of other nsLTPs. Douliez *et al*. reported that the dissociation constants for the two fatty acids are approximately 0.5 μM and that the number of binding sites ranges from 1.6 to 1.9 (10). These documented binding data are highly consistent with our data (Fig. 2).

The low solubility of WAX9D makes it difficult to carry out functional assays. Thus, we constructed Trx-WAX9D-conjugated protein to increase its solubility. Lipid-binding data for Trx-WAX9D indicate that the narrow binding spectrum of fatty acids to Trx-WAX9D is consistent with that to broccoli WAX9D, but that the binding affinities and the binding site number are altered slightly. Both broccoli WAX9D and Trx-WAX9D selectively binds two fatty acids, palmitate (C16) and stearate (C18), whereas other nsLTPs bind various fatty acids with chain lengths ranging from C12 to C18 (10). A distinct binding property of Trx-WAX9D is the larger number of lipid-binding sites ($n = 3$) compared to other nsLTPs, including broccoli WAX9D ($n < 2$). Given that the number of binding sites represents the size of the lipid-binding cavity, the lipid-binding cavity of Trx-WAX9D may be larger than that of other nsLTPs, including broccoli WAX9D. For example, the hydrophobic cavity of rice nsLTP2 is smaller than that of rice nsLTP1 (17). It still remains unknown whether and to what degree the Trx domain affects the lipid-binding properties of native WAX9D. However, our fluorescence data revealed that the Trx-tagged protein had little effect on monitoring the binding properties of WAX9D by means of fluorescence spectra (data not shown). Still, we cannot rule out structural interference of the Trx-tagged protein for the WAX9D domain.

One notable feature of the Trx-WAX9D protein is its binding specificity for palmitate. The binding affinity of Trx-WAX9D to palmitate (K_d ~1.1 μM) was comparable to that of other nsLTPs (10), whereas the binding affinity to stearate (K_d ~6.4 μM) was greatly diminished. This specific binding property will be utilized to assess palmitate-associated *in vivo* functions and *in vitro* biochemical activities. For instance, an elevated amount of free fatty acids, including palmitate, exists in patients with type 2 diabetes, inflammation, and cardiovascular disease (18-20). In endothelial cells, palmitate plays an important role in apoptotic and cell signaling pathways (14). Interestingly, our data indicate that Trx-WAX9D reverses the apoptotic function and regulation of cell signaling pathways induced by palmitate. Thus, our findings provide an insight into the diversity of biological applications of the Trx-WAX9D protein.

MATERIALS AND METHODS

Purification of Trx-tagged WAX9D

WAX9D cDNA was inserted into a thioredoxin (Trx) and histidine (His) fusion vector (pET-32a). Then the fusion plasmid was transformed to *Escherichia coli* BL21 (21). The transformed *E. coli* strains were grown overnight in Luria-Bertani (LB) medium containing 50 μg/mL ampicillin at 37°C. Harvested *E. coli* were lysed as previously described (22). For apoptosis assays, lipopolysaccharide in the purified protein was removed as previously described (23).

The Trx-untagged WAX9D protein was prepared by thrombin digestion of the Trx-WAX9D-Ni^{2+}-affinity bead complexes (24). Then the supernatant and bead fractions were resolved by 15% SDS-PAGE and detected by either Coomassie Brilliant Blue staining or western blotting with a polyclonal anti-WAX9D antibody (11).

Purification of WAX9D from broccoli leaves

Broccoli (*Brassica oleracea*) leaves were obtained from Angel Farm (Kongju, South Korea). Native WAX9D proteins were purified as previously described (11). Purified WAX9D was resolved by either 18% SDS-PAGE or native gel electrophoresis (25), and resolved proteins were detected by silver staining according to a previous report (26).

Fluorescence spectroscopy

Fluorescence spectra for WAX9D or its recombinant protein were obtained by using a Shimadzu RF-5301PC spectrofluorometer (Kyoto, Japan). Protein samples were excited at 275 nm, and emission spectra were obtained in the range of 290 to 380 nm. For binding assays with broccoli WAX9D, 0.9 μM of protein was placed in a cuvette, and a small volume of concentrated fatty acid solution was added to the cuvette in a stepwise manner. The fluorescence intensity for a mixture was obtained at 333 nm, and F was calculated according to Equation 1,

$$F = \{(F_0 - F_x)/F_0\} \times 100 \qquad (1)$$

where F_0 and F_x represent the fluorescence intensities of WAX9D, free and at various concentration of fatty acids, respectively. A nonlinear fitting procedure using the following equation (Equation 2) for binding of protein (WAX9D) to fatty acids (L) returns the dissociation constant (K_d) and the number of lipid-binding sites (n),

$$F = (F_{max} \times [L]^n)/(K_d + [L]^n) \qquad (2),$$

where F_{max} is the F value at fatty acid saturation. Data were fitted using Origin software (Microcal, Northampton, MA, USA).

For binding assays with the Trx-WAX9D protein, 3 μM of protein was placed in a cuvette, and a small volume of concentrated fatty acid solution was added to the cuvette in a stepwise manner. The fluorescence spectrum for a mixture was obtained, and the average wavelength ($<\lambda>$) was calculated according to Equation 3,

$$<\lambda> = \Sigma F_i\lambda_i / \Sigma F_i \qquad (3),$$

where F_i represents the fluorescence intensity at a specific wavelength, λ_i (27).

For nonlinear fits for binding of protein (Trx-WAX9D) to fatty acids (L), two different binding schemes were constructed. Based on a previous finding that nsLTP has two different binding modes within a single lipid-binding site (13), we built the first scheme (Scheme I),

$$\text{WAX9D} \cdot \text{L} \underset{K_{d1}}{\overset{+L}{\rightleftarrows}} \text{WAX9D} \underset{K_{d2}}{\overset{+L}{\rightleftarrows}} \text{WAX9D} \cdot \text{L}' \qquad \text{(Scheme I)},$$

where dissociation constants of this scheme were described as K_{d1} = [WAX9D][L]/[WAX9D · L], K_{d2} = [WAX9D][L]/[WAX9D · L']. The bound protein fraction (Y) can be described using Equation 4.

$$Y = [\text{bound protein}]/[\text{total protein}] \qquad (4)$$

θ can also be expressed as $(<\lambda> - <\lambda_{min}>)/(<\lambda_{max}> - <\lambda_{min}>)$, where $<\lambda_{min}>$ and $<\lambda_{max}>$ are representative for lipid-bound and unbound Trx-WAX9D, respectively. From Equations 3 and 4, an equation can be derived to describe the average wavelength $<\lambda>$.

$$<\lambda> = \{(K_{d1} + K_{d2})[L]/(K_{d1} + K_{d2})[L] + (K_{d1}K_{d2})\} (<\lambda_{max}> - <\lambda_{min}>) + <\lambda_{min}> \qquad (5)$$

Wheat and barley nsLTPs were previously revealed to have multiple lipid-binding sites (10). Based on the lipid binding of wheat nsLTP, we built another scheme (Scheme II) describing multiple bindings.

$$\text{WAX9D} + \text{nL} \underset{K_d}{\rightleftarrows} \text{WAX9D} \cdot \text{L}_n \qquad \text{(Scheme II)},$$

where the dissociation constant (K_d) equals $[WAX9D][L]^n/[WAX9D \cdot L_n]$ and Y represents $[L]^n/(K_d + [L]^n)$. Together, we derived an equation (Equation 6),

$$<\lambda> = \{(\lambda_{min} \times K_d) + (\lambda_{max} \times [L]^n)\}/(K_d + [L]^n) \qquad (6),$$

where n is the number of lipid-binding sites. Data were fitted using Origin software.

Induction of apoptosis

Apoptotic cells were identified via visual assessment of cell morphology, namely cell rounding and shrinking. Bovine aort-

ic endothelial cell (BAEC) apoptosis was induced via 200 μM palmitate, and other procedures were performed as previously described (28, 29). Morphological changes in nuclear chromatin were detected by staining with the DNA-binding fluorescent dye Hoechst 33258 (Sigma) as previously described (28).

Acknowledgement
The present research was supported by the research fund of Dankook University in 2008.

REFERENCES

1. Kader, J. C. (1996) Lipid transfer proteins in plants. *Annu. Rev. Plant Physiol. Plant Mol. Biol.* **47**, 627-654.
2. Sterk, P., Booij, H., Schellerkens, G. A., Van Kammen, A. and De vries, S. C. (1991) Cell-specific expression of the carrot EP2 lipid transfer protein gene. *Plant Cell* **3**, 907-921.
3. Olmedo, F. G., Molina, A., Segure, A. and Moreno, M. (1995) The defensive role of nonspecific lipid-transfer proteins in plants. *Trends Microbiol.* **3**, 72-74.
4. Lin, K. F., Liu, Y. N., Hsu, S. T., Samuel, D., Cheng, C. S., Bonvin, A. M. and Lyu, P. C. (2005) Characterization and structural analyses of nonspecific lipid transfer protein 1 from mung bean. *Biochemistry* **44**, 5703-5712.
5. Smolennars, M. M., Madsen, O., Rodenburg, K. W. and Van der Horst, D. J. (2005) Molecular diversity and evolution of the large lipid transfer protein superfamily. *J. Lipid Res.* **48**, 489-502.
6. Shin, D. H., Hwang, J. Y., Kim, K. K. and Suh, S. W. (1995) High-resolution crystal structure of the non-specific lipid transfer protein from maize seedings. *Structure* **3**, 189-199.
7. Chavolin, D., Douliez, J. P., Marion, D., Cohen-Addad, C. and Pebay-Peyroula, E. (1999) The crystal structure of a wheat nonspecific lipid transfer protein (ns-LTP1) complexed with two molecules of phospholipid at 2.1Å resolution. *Eur. J. Biochem.* **264**, 562-568.
8. Douliez, J. P., Michon, T., Elmorjani, K. and Marion, D. (2000) Structure, biological and technological functions of lipid transfer proteins and indolines, the major lipid binding proteins from cereal kernels. *J. Cereal Sci.* **32**, 1-20.
9. Lee, J. Y., Min, K., Cha, H., Shin, D. H., Hwang, K. Y. and Suh, S. W. (1998) Rice non-specific lipid transfer protein : the 1. 6Å crystal structure in the unliganded state reveals a small hydrophobic cavity. *J. Mol. Biol.* **276**, 437-448.
10. Douliez, J. P., Michon, T. and Marion, D. (2000) Steady-state tyrosine fluorescence to study the lipid-binding properties of a wheat non-specific lipid-transfer protein (ns-LTP). *Biochim. Biophys. Acta.* **1467**, 65-72.
11. Pyee, J., Yu, H. and Kolattukudy, P. E. (1994) Identification of a lipid transfer protein as the major protein in the surface wax of broccoli (*Brassica oleracea*) leaves. *Arch. Biochem. Biophys.* **311**, 460-468.
12. Smialowski, P., Martin-Galiano, A. J., Mikolajka, A., Girschick, T., Holak, T. A. and Frishman, D. (2007) Protein solubility: sequence based prediction and experimental verification. *Bioinformatics* **23**, 2536-2542.
13. Cheng, H. C., Cheng, P. T., Peng, P., Lyu, P. C. and Sun, Y. J. (2004) Lipid binding in rice nonspecific lipid transfer protein-1 complexes from Oryza sativa. *Protein Sci.* **13**, 2304-2315.
14. Guerbette, F., Grosbois, M., Jolliot-Croquin, A., Kader, J. C. and Zachowski, A. (1999) Comparison of lipid binding and transfer properties of two lipid transfer proteins from plants. *Biochemistry* **38**, 14131-14137.
15. Chai, W. and Liu, Z. (2007) p38 mitogen-activated protein kinase mediates palmitate induced apoptosis but not inhibitor of nuclear factor-κB degradation in human coronary artery endothelial cells. *Endocrinology* **148**, 1622-1628.
16. Cho, K. H., Kim, S. T. and Kim, Y. K. (2007) Purification of a pore-forming peptide toxin, tolaasin, produced by *Pseudomonas tolaasii* 6264. *J. Biochem. Mol. Biol.* **40**, 113-118.
17. Cheng, C. S., Chen, M. N., Lai, Y. T., Chen, T., Lin, K. F., Liu, Y. J. and Lyu, P. C. (2008) Mutagenesis study of rice nonspecific lipid transfer protein 2 reveals residues that contribute to structure and ligand binding. *Proteins* **70**, 695-706.
18. Kahn, B. B. and Flier, J. S. (2000) Obesity and insulin resistance. *J. Clin. Invest.* **106**, 473-481.
19. Ginsberg, H. N. (2000) Insulin resistance and cardiovascular disease. *J. Clin. Invest.* **106**, 453-458.
20. Meshkini, A. and Yazdanparast, R. (2007) Induction of megakaryotic differentiation in chronic myelogenous leukemia cell K562 by 3-hydrogenkwadaphnin. *J. Biochem. Mol. Biol.* **40**, 944-951.
21. Pyee, J. and Kolattukudy, P. E. (1995) The gene for the major cuticular wax-associated protein and three homologous genes from broccoli (*Brassica oleracea*) and their expression patterns. *Plant J.* **7**, 49-59.
22. Kim, J., Shin, J. and Park, H. (2003) Structural characterization for N-terminal domain of caveolin-1. *Korean J. Biol. Sci.* **7**, 207-211.
23. Park, H., Park, S. G., Kim, J., Ko, Y. -G. and Kim, S. (2002) Signaling pathways for TNF production induced by human aminoacyl-tRNA synthetase-associated factor, p43. *Cytokine* **20**, 148-153.
24. Shin, J., Cho, M., Hyun, J. W., Pyee, J. and Park, H. (2006) A new method for immobilization of lipid-binding proteins to the glass slides. *Curr. Appl. Phys.* **6**, 271-274.
25. Hames, B. D. and Rickwood, D. (1981) *Gel electrophoresis of proteins*, IRL Press, Washington D. C., USA.
26. Chevallet, M., Luche, S. and Rabilloud, T. (2006) Silver staining of proteins in polyacrylamide gels. *Nat. Protoc.* **1**, 1852-1858.
27. Strader, M. B., Smiley, R. D., Stinnett, L. G., Verberkmoes, N. C. and Howell, E. E. (2001) Role of S65, Q67, I68, and Y69 residues in homoteterameric R67 dihydrofolate reductase. *Biochemistry* **40**, 11344-11352.
28. In, K. M., Park, J. B. and Park, H. (2006) Resveratol at high doses acts as an apoptotic inducer in endothelial cells. *Cancer Res. Treat.* **38**, 48-53.
29. Park, H., Go, Y. M., John, P. L., Maland, M. C., Lisanti, M. P., Abrahamson, D. R. and Jo, H. (1998) Plasma membrane cholesterol is a key molecule in shear stress-dependent activation of extracellular signal-regulated kinase. *J. Biol. Chem.* **273**, 32304-32311.